Contrib Mineral Petrol (1984) 86:159–169

Contributions to Mineralogy and Petrology
© Springer-Verlag 1984

Esmeralda Bank: Geochemistry of an active submarine volcano in the Mariana Island Arc

Robert J. Stern[1, *] **and L.D. Bibee**[2]

[1] Department of Terrestrial Magnetism, Carnegie Institution of Washington, Washington, DC 20015, USA
[2] School of Oceanography, Oregon State University, Corvallis, Oregon 97331, USA

Abstract. Esmeralda Bank is the southernmost active volcano in the Izu-Volcano-Mariana Arc. This submarine volcano is one of the most active vents in the western Pacific. It has a total volume of about 27 km^3, rising to within 30 m of sea level. Two dredge hauls from Esmeralda recovered fresh, nearly aphyric, vesicular basalts and basaltic andesites and minor basaltic vitrophyre. These samples reflect uniform yet unusual major and trace element chemistries. Mean abundances of TiO_2 (1.3%) and FeO* (12.6%) are higher and CaO (9.2%) and Al_2O_3 (15.1%) are lower than rocks of similar silica content from other active Mariana Arc volcanoes. Mean incompatible element ratios K/Rb(488) and K/Ba(29) of Esmeralda rocks are indistinguishable from those of other Mariana Arc volcanoes. On a Ti–Zr plot, Esmeralda samples plot in the field of oceanic basalts while other Mariana Arc volcanic rocks plot in the field for island arcs.

Incompatible element ratios K/Rb and K/Ba and isotopic compositions of Sr ($^{87}Sr/^{86}Sr = 0.70342 - 0.70348$), Nd ($\varepsilon_{Nd} = +7.6$ to $+8.1$), and O ($\delta^{18}O = +5.8$ to $+5.9$) are incompatible with models calling for the Esmeralda source to include appreciable contributions from pelagic sediments or fresh or altered abyssal tholeiite from subduction zone melting. Instead, incompatible element and isotopic ratios of Esmeralda rocks are similar to those of intra-plate oceanic islands or "hot-spot" volcanoes in general and Kilauean tholeiites in particular. The conclusion that the source for Esmeralda lavas is an ocean-island type mantle reservoir is preferred.

Esmeralda Bank rare earth element patterns are inconsistent with models calling for residual garnet in the source region, but are adequately modelled by 7–10% equilibrium partial melting of spinel lherzolite. This is supported by consideration of the results of melting experiments at 20 kbars, 1,150° C with CO_2 and H_2O as important volatile components. These experiments further indicate that low MgO (4.1%), MgO/FeO*(0.25) and Ni(12 ppm) in Esmeralda Bank melts are characteristic of initial melts generated by moderate degrees of melting of hydrous and carbonated mantle. Consideration of experimental determinations and spinel-lherzolite to garnet-lherzolite stabilities indicates Esmeralda Bank melts were generated by partial melting within the upper 60–110 km of the mantle.

Introduction

It is now clear that in order to understand the processes responsible for generating melts in and above subduction zones, it is necessary to study fresh igneous rocks from island arcs built on primitive oceanic crust (intra-oceanic arcs). Only in this way can the possible contribution of a low-melting fraction from sediments or continental crust

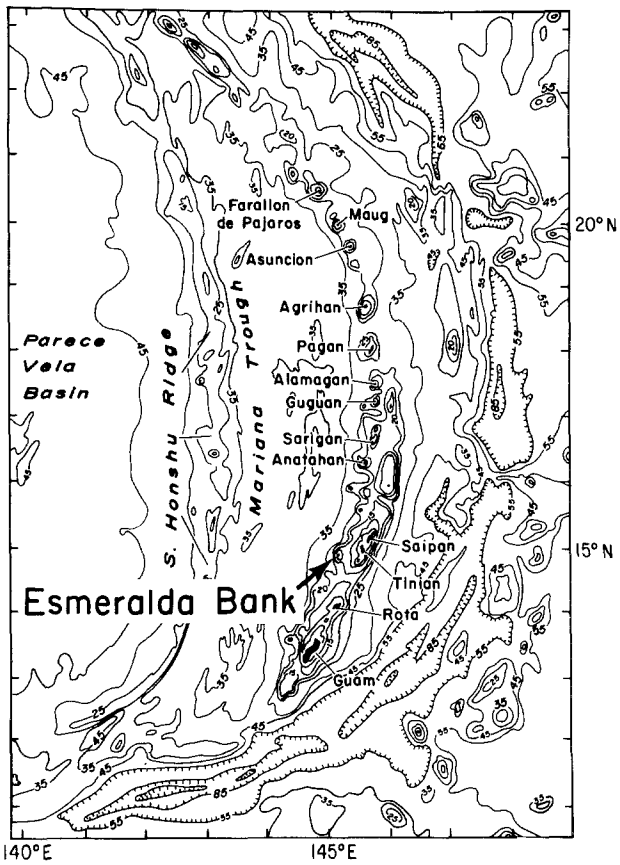

Fig. 1. Locality map of Esmeralda Bank in the Mariana Arc (modified after Meijer, 1976). Bathymetry in hundreds of meters

* *Present address:* Programs in Geosciences, The University of Texas at Dallas, Box 830688, Richardson, TX 75083-0688, USA

Offprint requests to: R.J. Stern

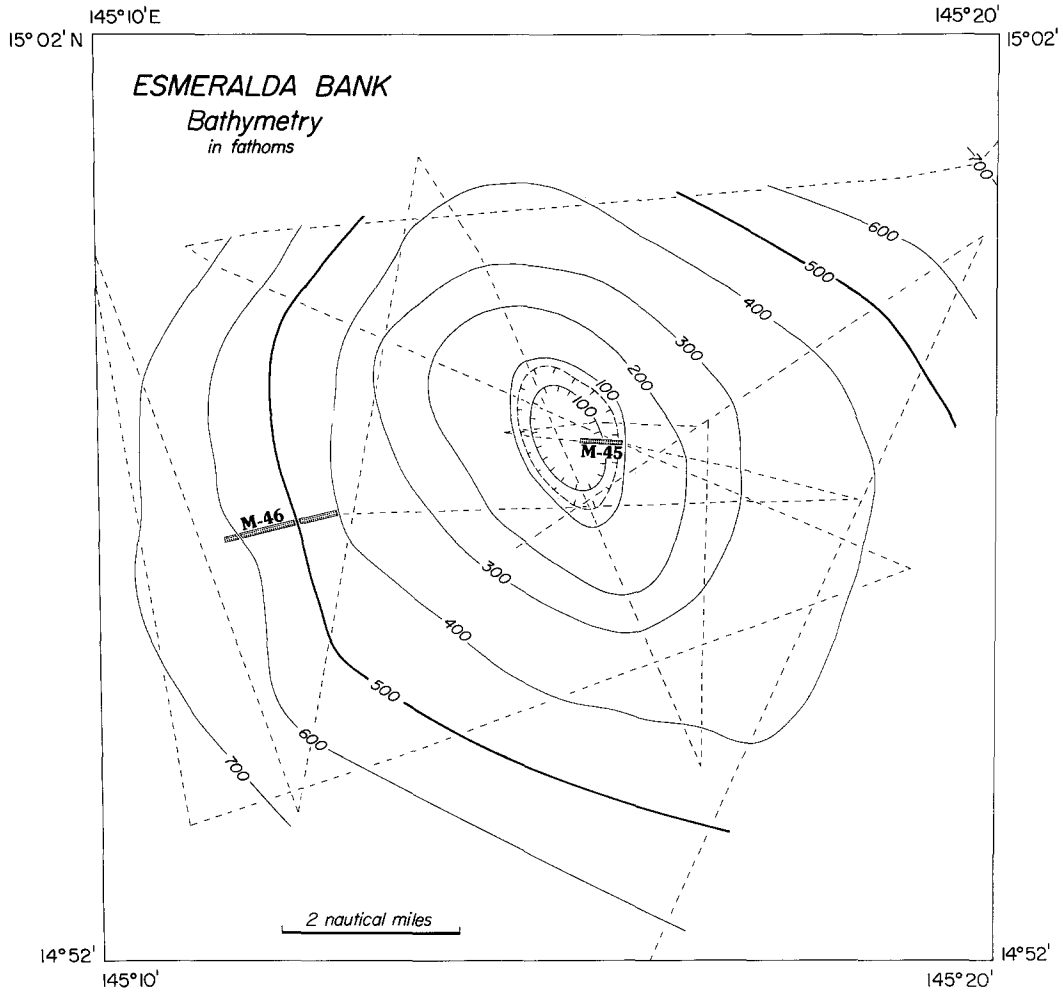

Fig. 2. Bathymetry of Esmeralda Bank based on detailed survey by *R/V Thomas Washington*. Ship tracks are shown as dashed lines. Inferred bottom contact of dredge is shown in stippled pattern. Note that the central crater is elongated towards the NW, crudely parallel to the line of the "boiling spots" of the 1975 eruption

just beneath the volcano be precluded. Petrologic investigations of intra-oceanic arcs are thus becoming increasingly comprehensive and detailed. To date, these have focussed on volcanic edifices developed above sea level. Submarine arc volcanoes are generally much smaller and thus probably represent more primitive stages of arc development. For this reason, confident reconstruction of arc magmatic evolution and petrogenesis requires consideration of the product of submarine vents. In spite of this, petrologic data from submarine arc volcanoes is limited (Corwin and Tracey 1965; Brothers 1967; Garcia et al. 1979; Brothers et al. 1980; Stern and Bibee 1980; Dixon and Stern 1983).

This paper reports the results of marine geophysical surveys and geochemical and isotopic investigations of basalts dredged from Esmeralda Bank, an active submarine volcano at the southern end of the volcanically active Mariana Arc (Fig. 1). Esmeralda Bank is among the most active volcanoes in the Marianas. Submarine eruptions, manifested at the surface as "sulphur boils", were reported in 1944 (Hess 1948) and 1975 (Ronck 1975). Esmeralda Bank rises 1,300 m above the Mariana Ridge to within 30 m of the sea surface. A central caldera, 300 m deep and 2 km across, dominates the volcanic structure. The basal diameter of the cone is about 9 km, indicating a volume of about 27 km^3. This is much less than the total volume of subaerial Mariana volcanoes, such as Agrigan ($\sim 10^3$ km^3; Stern 1979).

In December 1978 the R/V *Thomas Washington* surveyed the Esmeralda volcano (Fig. 2). Two dredges were made; one at 100–300 m depth from the eastern wall of the central crater and another at 800–1,200 m depth on the western flank. Samples recovered from the central crater (M-45) include volcanic flows, breccias, vitrophyre, and angular gabbroic fragments. Samples recovered from the flanks (M-46) make up a more homogeneous population of fresh vesicular basalts.

Analytical Techniques

Four samples from the crater wall and six samples from the western flank were selected for geochemical study. Only fresh, aphyric samples were selected. These criteria were easily satisfied; samples recovered from the west flank are nearly pristine and aphyric. Micro-phenocrysts of labradorite, clinopyroxene, and olivine make up less than 5% of these black, vesicular rocks. Samples recovered from the crater are more commonly altered and encrusted with small corals and other calcareous metazoa. Two samples of unaltered, aphyric basalt (M-45-10, 11) no doubt represent part of the upper 300 m of the volcanic stratigraphy. Fragments

Table 1.

	M-45 (Crater wall)				M-46 (Western flank)						Analytical error[c]	Esmeralda Bank mean composition
	G-1[a]	G-2[b]	10	11	1	2	3	10B	10T	11		
SiO_2	52.1	51.0	52.3	51.9	53.6	52.8	52.9	53.1	52.2	53.8	1.17	52.4
TiO_2	1.41	1.17	1.35	1.35	1.37	1.23	1.36	1.36	1.35	1.10	0.05	1.29
Al_2O_3	14.4	16.9	14.5	15.2	14.2	14.7	14.6	14.6	14.4	17.5	0.43	15.1
FeO*[d]	13.89	11.58	13.49	12.99	13.03	12.23	12.13	13.31	13.14	10.27	0.28	12.61
MnO	0.13	0.20	0.22	0.23	0.22	0.23	0.23	0.23	0.23	0.20	0.02	0.22
MgO	4.22	3.57	4.78	3.96	3.72	4.00	4.48	4.06	4.48	3.71	0.15	4.13
CaO	9.03	10.15	8.72	9.13	8.42	8.41	9.28	9.10	9.14	10.45	0.20	9.16
Na_2O	3.3	3.0	3.4	3.4	3.7	3.7	3.3	2.9	3.3	3.2	0.15	3.3
K_2O	1.07	0.90	0.89	0.99	1.01	0.95	0.91	0.92	0.92	0.72	0.08	0.92
P_2O_5	0.20	0.19	0.22	0.23	0.27	0.24	0.22	0.21	0.22	0.16	0.014	0.21
SUM	99.85	98.66	99.87	99.38	99.54	98.49	99.41	99.79	99.38	101.11		99.34
CIPW norms[e]												
Q	0.03	0.98	0.08	0.16	2.09	1.30	2.03	3.95	0.71	3.50		
OR	6.32	5.32	5.26	5.85	5.97	5.61	5.38	5.44	5.44	4.26		
AB	27.92	25.39	28.77	28.77	31.31	31.31	27.92	24.54	27.92	27.08		
AN	21.32	29.99	21.68	23.29	19.16	20.70	22.34	24.10	21.76	31.26		
DI	18.70	16.10	16.91	17.28	17.62	16.36	18.63	16.59	18.60	16.33		
HY	19.71	15.53	21.40	18.23	17.47	17.63	17.32	19.40	19.17	13.52		
OL												
MT	2.90	2.90	2.90	2.90	2.90	2.90	2.90	2.90	2.90	2.90		
IL	2.68	2.22	2.56	2.56	2.60	2.34	2.58	2.58	2.56	2.09		
AP	0.46	0.44	0.51	0.53	0.63	0.56	0.51	0.49	0.51	0.37		
Normative Plagioclase	An_{43}	An_{54}	An_{43}	An_{45}	An_{38}	An_{40}	An_{44}	An_{50}	An_{44}	An_{54}		
$\frac{K_2O}{Na_2O+K_2O}$	0.24	0.23	0.21	0.23	0.21	0.20	0.22	0.24	0.22	0.18		
$\frac{MgO}{FeO^*+MgO}$	0.23	0.24	0.26	0.23	0.22	0.25	0.27	0.23	0.25	0.27		
Color Index	44.0	36.8	43.8	41.0	40.6	39.2	41.4	41.5	43.2	34.8		

[a] Glass separate from plagioclase vitrophyre
[b] Whole-rock vitrophyre
[c] Analytical error defined as $2\sigma_{95}$ to working curve
[d] $FeO^* = FeO + 0.9\ Fe_2O_3$
[e] CIPW norms calculated assuming 2.00% Fe_2O_3

of fresh brown vitrophyre with 20–30% labradorite and 1% olivine phenocrysts were also analyzed (M-45-G1, G2).

Sample preparation focussed on removing adsorbed sea water; samples were slabbed and dried before they were ultrasonically rinsed, consecutively, in dilute HNO_3, distilled water, and acetone and dried at 110° C. Slabs were pulverized in a SPEX tungsten-carbide ball mill. Combined XRF and AA techniques were used for major element analyses as outlined by Stern (1979).

Nine samples were analyzed for Rb, Sr, Ba, Zr, and Ni by XRF. Four of these and USGS standard BCR were also analyzed for K, Rb, Sr, Cs, Ba, and REE by isotope dilution (ID) after the methods of Hart (1971) and Shimizu (1974a) (Table 3).

Comparison of analytical results by XRF and ID techniques are good with the exception of Ba. Abundances of this element as determined by XRF are consistently as much as 17% lower than determinations by ID on the same element. The reason for this discrepancy is unknown but is probably related to the fact that a relatively weak L_β line was used in XRF analysis. Since ID analysis of Ba in standard rock BCR is in good agreement with the preferred value of Flanagan (1973), it is expected that Ba concentrations determined by this method are more accurate.

Five samples were analyzed for $^{87}Sr/^{86}Sr$ and $^{143}Nd/^{144}Nd$. Sr isotopic analyses were performed as outlined in Stern (1982). Samples for which $^{143}Nd/^{144}Nd$ was originally reported in Stern and Bibee (1980) were re-analyzed at DTM following techniques outlined in Ishizaka and Carlson (1983). While an improvement in the accuracy and precision of the data is noted, the newer data do not significantly alter the conclusions of Stern and Bibee (1980).

Major Element Geochemistry

Major element compositions are listed in Table 1 along with estimates of analytical precision and a mean composition of the Esmeralda Bank samples. Several aspects of these data are noteworthy. First, the Esmeralda Bank samples are compositionally uniform. Silica ranges from 51.0 to 53.8%, spanning the limit of 52% silica taken to divide basalts from basaltic andesites (Jakes and White 1972). This is similar to the mode of 50–52% silica found for volcanic

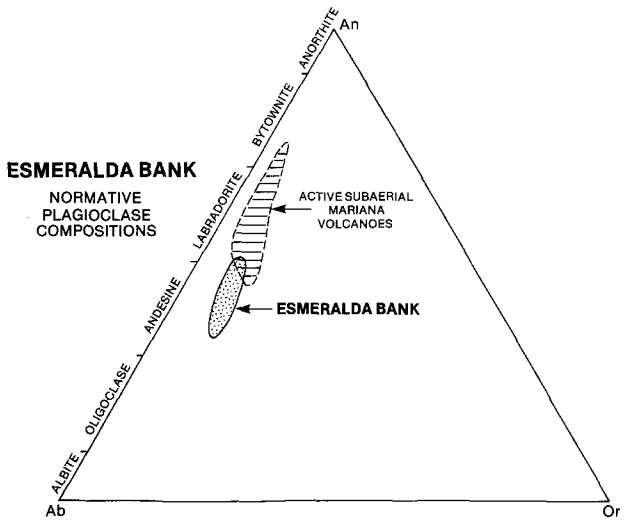

Fig. 3. Normative plagioclase composition of Esmeralda Bank samples compared with similar samples ($\leqq 55\%$ SiO_2) from the active subaerial Mariana Arc (Larson et al. 1974; Dixon and Batiza 1979; Stern 1979 and unpubl. data)

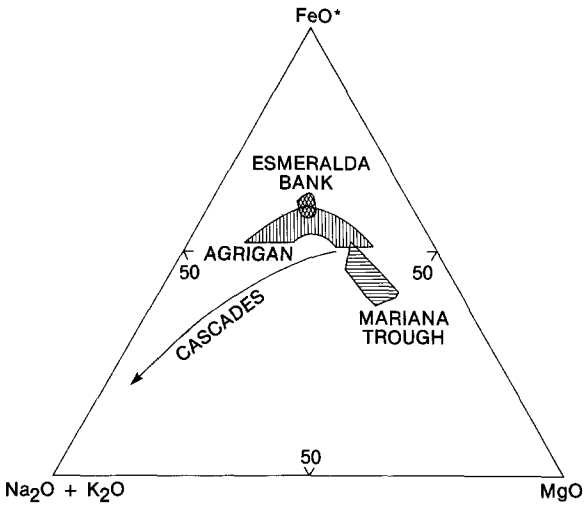

Fig. 4. AFM diagram for Esmeralda Bank volcanic rocks. Also shown is the field defined by the fractionation trend of basalt to andesite from Agrigan (Stern 1979), the Cascade or calc-alkaline fractionation sequence, and the field occupied by Mariana Trough rocks recovered during the TASADAY expedition (Stern, unpubl. data). Note that Fe-enrichment in Esmeralda Bank samples, while absolutely greater than any other Mariana Arc volcano, is relatively limited in its range

rocks of the subaerial Mariana Arc (Larson et al. 1974; Dixon and Batiza 1979).

Other major elements, however, differ slightly from "typical" Mariana basalts and basaltic andesites. Lavas from the active Mariana Arc with less than 54% SiO_2 typically contain 15.5–21.4% Al_2O_3 as compared to 14.2–17.5% for Esmeralda Bank (Larson et al. 1974; Stern 1979 and unpublished data; Dixon and Batiza 1979). Calcium abundances are also less in the Esmeralda Bank basaltic and basaltic andesites (EBB) (8.41–10.45% CaO) as compared with other Mariana basalts and basaltic andesites (MBBA) (8.8–13.3% CaO) while Na_2O is higher in EBB (2.9–3.7% vs. 2.3–3.2% in MBBA). These variations are manifested by the presence of labradorite phenocrysts in EBB (Dixon and Stern 1983) as compared with anorthite and bytownite in MBBA, and in the more sodic nature of EBB normative plagioclase (Table 1, Fig. 3).

Ferromanganese element concentrations are especially high in Esmeralda Bank flows relative to those of other Mariana Arc volcanoes. Iron expressed as ferrous oxide (FeO*) from MBBA ranges from 8.1–12.1% as compared to 10.3–13.9% for EBB. MnO in MBBA (0.03–0.22%) is less than EBB (0.20–0.23%). Concentrations of TiO_2 in EBB are typically 10–50% greater than MBBA lavas. With one exception (analysis 8 of Larson et al. 1974; $TiO_2 = 1.5\%$), Mariana Arc basalts and basaltic andesites contain 0.49–1.06% TiO_2 vs. 1.10–1.4% in Esmeralda Bank. The extent of Fe–Ti–Mn enrichment is emphasized in an AFM diagram (Fig. 4), which shows EBB to have greater Fe-enrichment than the most Fe-rich rocks of Agrigan, heretofore thought to represent the greatest degree of Fe-enrichment in the Marianas (Stern 1979).

Incompatible elements P and K are generally more enriched in EBB than are those from MBBA (K_2O: 0.79–1.07% vs. 0.37–1.20%; P_2O_5: 0.16–0.27% vs. 0.01–0.25%).

Trace element geochemistry

K, Rb, Sr, Cs, Ba

The absolute abundances of K, Rb, Sr, and Ba in Esmeralda Bank samples are very similar to the "average N. Mariana lava" of Chow et al. (1980), although these averages are weighted by andesites with up to 60% SiO_2. Potassium ranges from 5,620–7,620 ppm compared to 6,900 ppm for the average N. Mariana lava, while Rb varies from 11.52–15.60 ppm vs. 14.8 ppm. Sr and Ba are slighty enriched in Esmeralda samples (303–385 ppm vs. 304 ppm; 217–270 ppm vs. 219 ppm). Cs abundances are somewhat greater in Esmeralda Bank samples (0.50–0.95 ppm) as compared with other Mariana samples (0.19–0.60 ppm; Dixon and Batiza 1979). Incompatible element ratios are also similar to those of other Mariana Arc samples. K/Rb in Esmeralda Bank samples range from 472–517 as compared with an average of 493 for the N. Marianas (Chow et al. 1980). K/Ba ranges from 24.1 to 31.9 as compared with a N. Mariana average of 31.2. K/Cs varies from 6,500 to 14,000, somewhat lower than the range of 11,000 to 28,000 found for other Mariana Arc lavas (Dixon and Batiza 1979). In most respects, the relative and absolute abundances of incompatible elements in EBB are similar to those of other volcanoes of the Mariana Arc.

Ni and Zr

Abundance of Ni in Esmeralda Bank samples is uniformly low (9–17 ppm). This is typical of most Mariana Arc lavas, although Dixon and Stern (1983) found that aphyric Zealandia Bank basalts contained up to 100 ppm Ni. With this exception, Mariana Arc volcanic rocks contain less than 40 ppm Ni (Stern 1979; Dixon and Batiza 1979; Meijer and Reagan 1981; Wood et al. 1981; Dixon and Stern 1983).

Zirconium concentrations in EBB range from 72 to 96 ppm in Esmeralda Bank samples. This is similar to the range reported for other lavas from volcanic islands and seamounts of the northern Mariana Arc (Stern 1979; Meijer

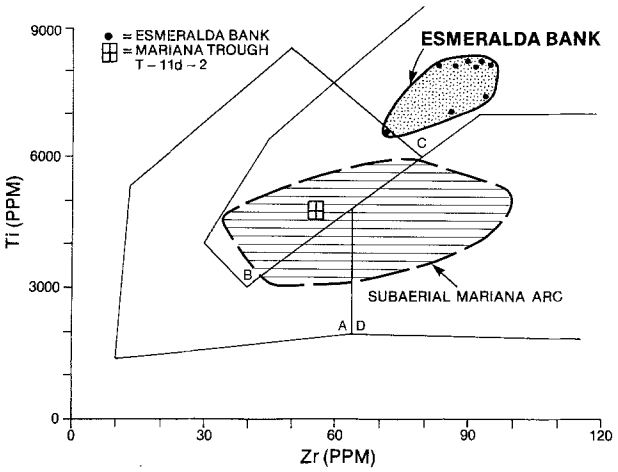

Fig. 5. Ti–Zr discriminant diagram after Pearce and Cann (1973), with data plotted from Esmeralda Bank and subaerial Mariana Arc (Meijer 1974; Stern 1979). Ocean-floor basalts plot in fields B and C, arc tholeiites plot in fields A and B, and calc-alkaline rocks plot in fields A, B, and D. Note that while volcanic rocks from the subaerial Mariana Arc plot within the arc field, samples from Esmeralda Bank plot in the field for ocean-floor basalts. Included for comparison is T-11d-2 from the Mariana Trough (Stern unpubl data)

and Reagan 1981; Wood et al. 1981; Dixon and Stern 1983). Mean Ti/Zr in EBB is 87 ± 6 (1 S.D.), significantly higher than volcanic rocks from Sarigan ($\bar{X} = 63 \pm 11$, Meijer and Reagan 1981), Fukujin ($\bar{X} = 71 \pm 9$, Wood et al. 1981), and other Mariana Arc seamounts ($\bar{X} = 63 \pm 20$; Dixon and Stern 1983). On Ti–Zr plots used to distinguish island arc from MORB and intra-plate basalts (Fig. 5) EBB plot in the MORB field. This contrasts with other samples of the Mariana active arc, which plot in the field of convergent-margin volcanic rocks (Meijer 1974; Stern 1979). This emphasizes the unusual geochemistry of Esmeralda Bank lavas and shows that such diagrams, while often useful, cannot be relied upon to unequivocally discriminate among igneous rocks of different tectonic environments.

Rare earth elements (REE)

Four Esmeralda Bank basalts and basaltic andesites were analyzed for REE (Table 3). These results have been normalized to chondritic abundances and plotted (Fig. 6). The samples are enriched in light REE with chondrite-normalized Ce/Yb ($(Ce/Yb)_N$) of 1.61–1.84 and Sm/Nd of 0.274–0.290. There are no significant europium anomalies, suggesting that extensive plagioclase fractionation has not occurred. The Esmeralda Bank samples are similar to basalts and basaltic andesites of subaerial Mariana Arc volcanoes ($(Ce/Yb)_N = 0.58$–2.08; Dixon and Batiza 1979). REE patterns for Esmeralda Bank basalts are significantly enriched in light REE as compared with representatives of island arc tholeiites (Jakes and Gill 1970).

Sr and Nd Isotopic Composition

Five samples analyzed for Nd and Sr isotopic composition showed no significant variations (Table 4). Mean $^{87}Sr/^{86}Sr$ of 0.70346 ± 4 is indistinguishable from the mean for the Mariana Arc (0.70342 ± 14) listed by Stern (1982). Neodymium isotopic compositions are similarly restricted to $\varepsilon_{Nd} = 7.8 \pm 0.3$, similar to those reported by DePaolo and Wasserburg (1977), Stern (1981), and Dixon and Stern (1983), as well as one arc tholeiite analyzed by Hickey and Frey (1982).

Table 2. XRF data for Rb, Sr, Ba, Zr, and Ni

		Rb	Sr	Ba	Zr	Ni
Dredge	M-45:					
	G-2	15	377	195	87	11
	10	11	335	265	93	15
	11	16	336	240	96	10
Dredge	M-46:					
	1	18	356	249	94	9
	2	15	318	210	95	10
	3	14	318	234	84	12
	10					
	Top	15	326	223	88	17
	Bottom	16	332	229	91	12
	11	10	374	194	72	10
Error[a]		3	9	14	8	6

[a] Error defined as $2\sigma_{95}$ to the working curve

Table 3. Isotope dilution data for K, Rb, Sr, Cs, Ba, and REE in Esmeralda Bank basalts and USGS standard BCR

	M-45-G2	M-46-2	M-46-10B	M-46-11	BCR
K	6,960	7,621	7,367	5,620	14,130
Rb	14.67	14.73	15.60	11.52	47.40
Sr	377.0	303.0	337.6	385.0	329.0
Cs	0.50	0.65	0.95	0.86	0.96
Ba	218.9	239.1	270.0	233.2	682.0
Ce	17.25	18.34	20.14	15.61	53.9
Nd	12.01	13.26	14.39	11.35	28.54
Sm	3.29	3.74	4.17	3.25	6.45
Eu	1.20	1.34	1.46	1.21	2.00
Gd	3.97	4.14	4.90	4.00	6.67
Dy	4.00	4.70	5.02	4.02	6.06
Er	2.46	3.08	3.17	2.54	3.51
Yb	2.38	2.63	3.02	2.46	3.51
K/Rb	474	517	472	488	
K/Cs	13,937	11,797	7,755	6,505	
K/Ba	31.8	31.9	27.3	24.1	
Rb/Sr	0.039	0.049	0.046	0.030	
(Eu/Eu*)[a]	1.016	1.042	0.993	1.032	
$(Ce/Yb)_N$[b]	1.84	1.77	1.70	1.61	
Sm/Nd	0.274	0.282	0.290	0.286	
Sr/Nd	31.39	22.85	23.46	33.9	

[a] (Eu/Eu*) is the Europium Anomaly Index as defined by the abundance of Eu relative to that extrapolated from abundances of Sm and Gd (Eu*)

[b] $(Ce/Yb)_N$ is the chondrite-normalized relative abundance of Ce to Yb

Discussion: Source region of Esmeralda Bank basalts: Subducted slab or mantle wedge?

Following the general acceptance of the sea-floor spreading/plate tectonic hypothesis, petrologists have wondered about the origin of melts generated in or above subduction zones. These discussions have often been confused by failure to prove or lay to rest questions of crustal contamination. The intra-oceanic arcs in general and small submarine

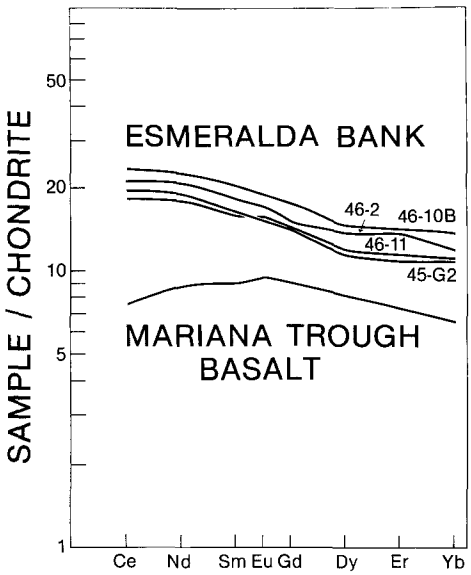

Fig. 6. Rare Earth Element patterns for Esmeralda Bank samples. Included for comparison is T-11d-2 from the Mariana Trough (Stern unpubl. data)

Table 4. Isotopic composition of Sr and Nd, Esmeralda Bank basalts and basaltic andesites

	$^{87}Rb/^{86}Sr$	$^{87}Sr/^{86}Sr$[a]	$^{147}Sm/^{144}Nd$	$^{143}Nd/^{144}Nd$[b]	ε_{Nd}
Dredge 45:					
G2	0.114	0.70342±7	0.166	0.51306±3	+8.1
Dredge 46:					
2	0.143	0.70346±6	0.171	0.51303±3	+7.7
10					
-Flow top	–	0.70346±6	–	0.51304±3	+7.8
-flow bottom	0.135	0.70348±3	0.175	0.51303±3	+7.6
11	0.088	0.70346±5	0.173	0.51305±2	+8.0

[a] Normalized to E & A $^{87}Sr/^{86}Sr = 0.70800$
[b] Normalized to UCSD Nd $^{143}Nd/^{144}Nd = 0.511860$

edifices in particular are situated in ideal crustal environments so that problems of crustal contamination should be negligible. In cases such as Esmeralda Bank, isotopic compositions of Sr and Nd should be the same as that of the source. In addition, the ratio of incompatible elements K, Rb, Cs, and Ba should be relatively unaffected by fractionation in crustal reservoirs which in the Izu-Mariana system typically involve pyroxene, olivine, calcic plagioclase, and magnetite (Isshiki 1958; Matsuhisa 1979; Stern 1979; Meijer and Reagan 1981; Dixon and Stern 1983). Pyroxene and olivine have distribution coefficients ($D^{XL/L}$) of less than 0.03 for these elements (Shimizu 1974b; Philpotts and Schnetzler 1970). Distribution coefficients for these elements between plagioclase and liquid are less than 0.23 (Arth 1976). Extensive fractionation leads to decreasing K/Rb (and K/Cs) and increasing K/Ba (Gunn 1965; Shaw 1968). Reported ratios, while probably quite close to that of the source regions, should nertheless be taken as lower limits for K/Rb and K/Cs and upper limits for K/Ba in the source. These data may then be used to compare the relative abundance of the incompatible elements in the source region of Esmeralda Bank with that of other basalt types. Table 5 lists values for incompatible element ratios for igneous rocks of Esmeralda Bank and the Marianas, "hot spot" volcanoes such as Hawaii, fresh and altered MORB, and oceanic sediments. Rb/Ba and K/Rb in Esmeralda and other Mariana lavas are similar to Kilauea and altered MORB but significantly different than fresh MORB and sediment. K/Ba in Esmeralda Bank and other Mariana lavas are 10–20% lower than for Kilauea but greatly different than of fresh or altered MORB or sediment. Comparison of strontium isotopic compositions also shows a similarity between the Marianas and Kilauea. The main difference between Esmeralda and Mariana Arc lavas and those of Kilauea is K/Cs, which in the Marianas is 20–45% that of Kilauea. This is the only incompatible element signature that is more similar to subducted crust than typical "hot spot" sources.

Similarities in incompatible element ratios between "hot spot" basalts and Mariana Arc lavas were emphasized by Chow et al. (1980) who argued for similar source compositions between intra-plate and Mariana Arc magmatism. These conclusions are substantiated by the Esmeralda Bank data. It is important to note, however, that mixing about 10% sediment with fresh and altered MORB could produce melts with K/Rb = 400, K/Cs = 4,600, K/Ba = 11, and $^{87}Sr/^{86}Sr \sim 0.7035$ (Hart et al. 1970). The argument that incompatible element ratios of Esmeralda Bank Basalts represents such mixing of sources cannot be evaluated on the basis of the incompatible element data alone. To resolve this question, consideration of the Sr and Nd isotopic results is required.

Volcanic rocks of the active Mariana Arc are remarkably uniform in their Sr-isotopic composition ($^{87}Sr/^{86}Sr = 0.70342 \pm 14$; Stern 1982). The total variation of $^{87}Sr/^{86}Sr$ in volcanoes from 500 km along the arc is less than 0.09%. This uniformity is even more remarkable when it is compared with isotopic variations from unequivocally mantle-derived "hot spot" volcanoes of the Pacific Basin. Total Sr-isotopic variation of 0.2% are observed for the Galapagos, Hawaii, or Samoa (White and Hofmann 1982; O'Nions et al. 1977; Hedge et al. 1972). Along a distance similar to that spanned by the Mariana Arc, the Society Islands show a variation in $^{87}Sr/^{86}Sr$ of 0.45% (Duncan and Compston 1976).

Models calling for the melting of subducted pelagic sediments as an important aspect of magmagenesis beneath island arcs are difficult to reconcile with the observed uniformity of $^{87}Sr/^{86}Sr$ in the Marianas. Sediments now being subducted beneath the Marianas are dominated by Cretaceous carbonates which contain 500–1,000 ppm Sr. The isotopic composition of Sr in Mesozoic carbonates is in the range 0.7070–0.7081 (Faure et al. 1978). The admixture of such material to typical mantle lherzolite ($Sr \sim 10$ ppm, $^{87}Sr/^{86}Sr \sim 0.703$) would result in significant increases of $^{87}Sr/^{86}Sr$ in resulting melts for very small additions of this sediment. For example, let us assume an unmodified mantle source has $^{87}Sr/^{86}Sr$ similar to that of Salt Lake Crater xenoliths (mean of 3 xenoliths = 0.7032; O'Neil et al. 1970). If we assume a mantle with 10 ppm Sr, then addition of 1% and 10% pelagic carbonate with 1,000 ppm Sr would produce a hybrid with $^{87}Sr/^{86}Sr = 0.7054$ and 0.7071, respectively. The uniformity of $^{87}Sr/^{86}$-Sr in Mariana Arc magmas thus requires that if mixing of Sr from subducted pelagic sediments with the overlying mantle wedge occurs,

Table 5. Mean incompatible element ratios for Esmeralda Bank and related Mariana Arc volcanic rocks and possible sources

	Mariana Arc		Mantle		Subducted crust	
	Esmeralda Bank	Subaerial Marianas	Hot spot Kilauea[b]	Fresh MORB[c]	Altered MORB[d]	Crust sediments[e]
K/Rb	488	493[a]	503	1,060	450	286
K/Ba	29	31[a]	36	110	230	7
K/Cs	10,000	20,500[f]	47,000	70,000	7,000	3,000
Rb/Ba	0.06	0.07[a]	0.07	0.11	0.51	0.03
$^{87}Sr/^{86}Sr$	0.70346	0.7034[g]	0.70352	0.7026	0.7034	~0.71

[a] Chow et al. 1980 [b] Hofmann et al. 1978 [c] Hart 1971 [d] Hart et al. 1974 [e] Hart et al. 1970
[f] Dixon and Batiza 1979 [g] Stern 1982

this must be an extremely uniform process, always limited to less than 1% sediment. For such a process to produce the uniform $^{87}Sr/^{86}Sr$ in Mariana lavas also requires mantle with less isotopic heterogeneity than that beneath Hawaii, etc. This kind of argument also applies if we consider the incompatible element ratios. Again, mixing of sediments with mantle should produce a much greater range of K/Rb, K/Ba, $^{87}Sr/^{86}Sr$, etc., than that observed as to make this an exceedingly unattractive model.

Combined Nd- and Sr-isotopic results are a powerful tool for the elucidation of source regions of island arcs. Oceanic igneous rocks manifest a strong inverse relationship between $^{143}Nd/^{144}Nd$ and $^{87}Sr/^{86}Sr$ such that the field of the sub-oceanic mantle can be confidently defined (O'Nions et al. 1977; DePaolo and Wasserburg 1976; Richard et al. 1976). This understanding can be used to evaluate the roles of mantle and subducted slab and sediments in the petrogenesis of island arc magmas. As outlined by DePaolo and Johnson (1979), melting of subducted oceanic crust and/or sediments should produce magmas with an isotopic signature displaced to the high $^{87}Sr/^{86}Sr$ side of the oceanic mantle array. Pelagic sediments, which may be subducted and melted along with MORB, also plot far to the right of Nd–Sr mantle array (O'Nions et al. 1978).

Data for Esmeralda Bank samples are plotted on a Nd–Sr diagram in Fig. 7. Also shown for comparison is the "oceanic mantle array" as defined by all analyses of fresh volcanic rocks of MORB and the intra-plate ocean islands. The fields occupied by altered and subducted Mesozoic MORB and pelagic sediments are shown as well. Comparison of the Esmeralda data with these source candidates indicates that the contribution of subducted material to Esmeralda Bank magmas is small. This is especially clear for the case of pelagic sediments, less so for subducted basaltic crust.

Finally, oxygen isotopic analyses indicate a mantle signature. Ito and Stern (1981) reported $\delta^{18}O$ of +5.8 and +5.9 for glassy samples M-45G and M-45-10T. These values are indistinguishable from mantle values.

Incompatible element ratios and isotopic data for Esmeralda Bank samples are thus most consistent with models calling for magmagenesis in the mantle overlying the subduction zone. The depth of melting within the 150 km of the upper mantle wedge can be considered using REE patterns of Esmeralda Bank volcanics (Fig. 8). This portion of the mantle should consist of peridotites in which Al_2O_3 is largely sequestered in spinel or, at greater depth, in garnet. That the upper mantle beneath circum-Pacific arcs and the Pacific Basin itself is dominated by such peridotites

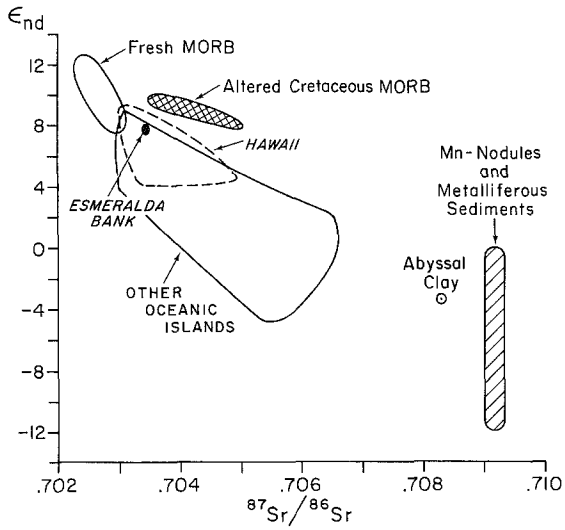

Fig. 7. $^{143}Nd/^{144}Nd$-$^{87}Sr/^{86}Sr$ plot of Esmeralda Bank samples and plausible source isotopic compositions. Data for each field are from the following sources: 1) Fresh MORB: DePaolo and Wasserburg 1976; O'Nions et al. 1977; Cohen et al. 1980; White and Hofmann 1982. 2) Ocean Island Tholeiites and Alkali Volcanic Rocks: DePaolo and Wasserburg 1976; O'Nions et al. 1977; White and Hoffman 1982; Zindler et al. 1979. 3) Altered Cretaceous MORB: McCulloch et al. 1980; Jahn et al. 1980. 4) Pelagic Red Clays, Mn-Nodules, and Metalliferous Sediments: McCulloch and Wasserburg 1978; O'Nions et al. 1978; Piepgras et al. 1979. The range of altered Cretaceous MORB is taken as an approximation to the isotopic composition of basaltic crust now being subducted beneath the Mariana Arc while the isotopic composition of Nd and Sr in red clay, Mn-nodules, and metalliferous dediments is taken to represent that of subducted sediments

has been shown by many studies. (e.g., Jackson and Wright 1970; Shimamura et al. 1976, 1977; Batiza 1977; Takahashi 1978; Nixon and Boyd 1979; Delaney et al. 1979; Tracey 1980; Frey 1980). Experimental investigations of spinel peridotite-garnet peridotite equilibrium indicate that, assuming an oceanic geothermal gradient (~35° C/kb), the subsolidus reaction 4 Enstatite + Spinel ⇌ Forsterite + Pyrope should occur at 18–22 kb (MacGregor 1964, 1974; Obata 1976; Danckwerth and Newton 1978). In nature, this reaction also depends on the presence of clinopyroxene and bulk concentrations of CaO and Cr_2O_3 and Al_2O_3 in spinel. Thus, at 1,200° C, the reaction natural spinel peridotite ⇌ garnet peridotite may occur between 18–33 kb, corresponding to mantle depths of 60 to 110 km (Ito and Kennedy 1967; Kushiro et al. 1968; MacGregor 1970).

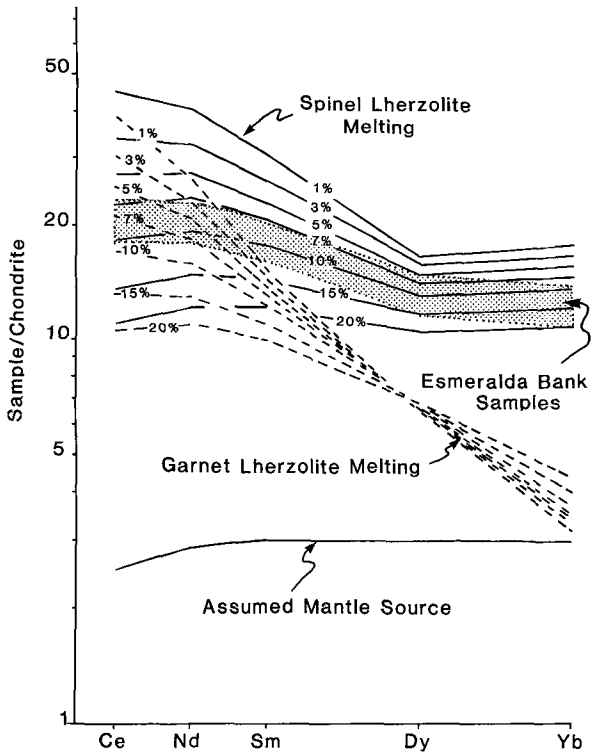

Fig. 8. Melting model for the generation of Esmeralda Bank lavas from the mantle, based on REE. Elements Sm through Yb are assumed 3 × chondritic in the source (Kay and Gast 1973). Nd/Sm determined from solution of radiogenic growth equation for

$$^{147}Sm/^{144}Nd = \frac{(^{143}Nd/^{144}Nd) - (^{143}Nd/^{144}Nd)_t}{e^{\lambda t} - 1}$$

where $(^{143}Nd/^{144}Nd)$ is the present mean value for Esmeralda Bank sample (0.5130), $t = 2 \times 10^9$ yrs for the suggested age of source, and $(^{143}Nd/^{144}Nd)$ is the value for the bulk earth at $t = 2 \times 10^9$ years ago. Ce is an extrapolation from Sm and Nd. Non-modal melting is assumed. Garnet lherzolite is assumed to be 50% OL, 25% OPX, 15% CPX, and 10% GAR; orthopyroxene, clinopyroxene, and garnet are assumed to melt in the proportions 3:3:2. Spinel lherzolite is assumed to be 55% OL, 25% OPX, 15% CPX, and 5% spinel; clinopyroxene and orthopyroxene melt in equal proportions. Distribution coefficients for olivine and orthopyroxene are from the experimental work of Mysen (1978) at 950–1,025° C, 20 kb. Distribution coefficients for clinopyroxene and garnet are from experimental studies of Nicholls and Harris (1980), at 1,380° C for the heavy REE, and at 1,240° C for Ce and Nd. Distribution coefficients ($D^{XL/L}$) for spinel are assumed to be zero. Expected REE contents of melts after 1, 3, 5, 7, 10, 15 and 20% equilibrium fusion are shown for melting of garnet lherzolite (dashed lines) and spinel lherzolite (solid lines). The equation

$$C_L = \frac{C_0}{D_0 + F(1-P)}$$

was used throughout. Also shown is the field occupied by Esmeralda Bank samples

If Esmeralda Bank lavas are mantle-derived, their REE should manifest equilibrium with either garnet lherzolite or spinel lherzolite. Results of modelling of REE patterns expected from equilibrium partial melting of garnet lherzolite and spinel lherzolite are shown in Fig. 8. These results indicate that garnet cannot be residual in the source of Esmeralda Bank magmas. Considering uncertainties of mantle mineralogy, bulk REE abundances in the source, proportions of phases melting, distribution coefficients, etc., the Esmeralda Bank lavas fit remarkably well with a model calling for their derivation by 7–10% partial melt of spinel peridotite upper mantle. From the previous discussion of garnet-peridotite and spinel-peridotite stabilities, this indicates their probable derivation from the upper 60–110 km of the mantle wedge.

The hypothesis that Esmeralda Bank melts are generated in the upper 60 km of the upper mantle can be further evaluated by comparison with the results of melting experiments. Anhydrous melting of peridotite can produce silica-saturated melts at pressures up to 5 kbars. At greater pressures incongruent melting of enstatite is unlikely and melts are olivine-normative (Green and Ringwood 1967). Experimental anhydrous melting experiments of synthetic pyrolite indicate that 7–10% melting in the spinel field would produce undersaturated, Mg-rich alkali olivine basalt (Jaques and Green 1980). These results show that the Esmeralda Bank melts could not have been generated by dry melting. Detailed geochemical studies of volatiles in rocks from a submarine Mariana arc volcano average over 1 wt % H_2O and 0.25% CO_2 in fresh glasses (Garcia et al. 1979). Hydrous as opposed to anhydrous melting seems more likely (Anderson 1982) and work of Garcia et al. (1979) indicate CO_2 is also an important volatile component ($X_{CO_2} = 0.1$–0.5). Under conditions of hydrous melting of spinel peridotite, initial melts are strongly silica-oversaturated (57–68% SiO_2), low in MgO (0.6–4.1% MgO) and thus are crudely andesitic (Kushiro et al. 1972; Mysen 1974; Mysen et al. 1974). While these investigators argue that this persists throughout the stability field of spinel peridotite, Nicholls (1974) argues that silica-saturated melts can be generated by hydrous melting only at depths of less than 35 km. The upper pressure limit for the generation of silica-saturated liquids via hydrous melting of peridotite is thus presently unresolved (see discussion between Geophysical Lab and ANU groups in Mysen et al. 1974) but there is a consensus that this occurs at least in the uppermost mantle, within the spinel-peridotite stability field. These compositions are nonetheless greatly oversaturated with silica as compared with Esmeralda Bank melts.

Decreasing f_{H_2O} and increasing f_{CO_2} at constant T, P results in the generation from the same parent of a continuum of magmatypes from andesite to nepheline basalt (Mysen and Boettcher 1975b). Melting of spinel peridotite at 20 kbar and 1,150° C with $X_{H_2O} = 0.40$ can produce a basaltic andesitic melt that is similar in most respects to Esmeralda Bank melts (Table 6). The low MgO (5.1%) in these experimental melts is comparable to Esmeralda Bank melts. Low MgO (and Ni?) in Esmeralda Bank and other Mariana Arc lavas thus may be a characteristic of initial melts and is not necessarily the result of the subsequent fractionation of olivine from a high MgO melt (Taylor et al. 1969; Hedge 1971). Discrepancies persist for CaO which is higher in the experimental melt as compared with EBB and for TiO_2, FeO*, Na_2O, and K_2O (and other incompatible elements?) which are lower. Some of these differences can be eliminated by calling on a slightly different peridotite starting material. For example, pyrolite contains 3.5 times as much TiO_2 as the Hawaiian spinel lherzolite (Ringwood 1966); melting pyrolite instead of the spinel lherzolite under identical conditions seems likely to produce a melt with TiO_2 similar to or greater than in EBB. Similarly, the lower CaO and higher alkalies in pyrolite as opposed to the Hawaiian

Table 6.

	Esmeralda Bank, Mean composition[a]	Experimental melt Peridotite $+H_2O$ $+CO_2$[b]	Spinel-Peridotite[c]	Pyrolite[d]
SiO_2	52.4	53.7	43.7	45.2
TiO_2	1.29	0.6	0.20	0.71
Al_2O_3	15.1	15.2	4.0	3.54
$FeO*$	12.61	9.0	8.89	8.47
MnO	0.22	0.2	0.12	0.14
MgO	4.13	5.1	37.4	37.5
CaO	9.16	13.5	3.50	3.08
Na_2O	3.3	2.5	0.38	0.57
K_2O	0.92	0.1	0.01	0.13
P_2O_5	0.21	–	<0.01	–
SUM	99.34	100.0	98.20	99.34

[a] From Table 1

[b] Melt produced by melting Hawaiian spinel lherzolite. $P=20$ kb, $T=1{,}150°$ C $X^v_{H_2O}=0.40$; $X^v_{CO_2}=0.60$. Buffer = magnetite-hematite (Mysen and Boettcher 1975b)

[c] Hawaiian spinel peridotite, starting material for melting experiment, Mysen and Boettcher (1975a), Table 1, Column B

[d] Pyrolite model mantle composition (Ringwood 1966)

spinel peridotite should produce melts more similar to EBB under the same experimental conditions. This suggests that the spinel-peridotite mantle source for Esmeralda Bank melts may be grossly pyrolitic in its major-element composition.

Conclusion

Data presented here on the geochemistry and isotopic composition of Esmeralda Bank samples illuminate related problems of the origin and nature of arc volcanism in general and the more poorly understood field of submarine arc volcanism in particular. Compositional features of Esmeralda Bank basalts and basaltic andesitic indicate their ultimate source lay in the mantle. The source is almost indistinguishable from that of ocean island or "hot spot" basalts. High Ti and Fe, location on Ti – Zr diagram, low incompatible element radios K/Ba and K/Rb, and isotopic compositions of Sr and Nd are remarkably similar between the fresh flows of Esmeralda and Kilauea, Hawaii. With the exception of low K/C,s there is no obvious indication that any subducted material, either fresh or altered MORB or pelagic sediments, was involved in magmagenesis.

Esmeralda Bank basaltic and basaltic-andesitic rocks are distinct from those of other active Mariana Arc volcanoes in their high Ti and Fe, low Al, and location on Ti – Zr diagram. The cause of this difference is presently unresolved and may lie either in source compositional variations or differences in melting conditions, especially volatile fugacities. The latter might reflect differences in the subduction mechanism, since the deep seismicity of the N. Marianas is replaced by shallow and intermediate depth seismicity to the south. Nevertheless, similarities of K/Rb, K/Ba, $^{87}Sr/^{86}Sr$, and $^{143}Nd/^{144}Nd$ indicate significant common source characteristics exist for Esmeralda Bank and other active Mariana Arc volcanic rocks. In this regard, conclusions regarding the Esmeralda Bank source region may hold for the entire active Mariana Arc. It seems less likely that these conclusions hold true for all arcs, but that magmagenesis varies from arc to arc. Some arc magmas may be largely derived from melts or metasomatic fluids released from subducted crust while others are almost totally derived from the mantle.

A final note: the recognition that some island arc magmas are derived from an "ocean-island" type mantle source indicates that these less-depleted sources must lie, at least partly, within the top 150 km of the upper mantle. In the case of Esmeralda, this source appears to extend to within 60–110 km of the earth's surface. This information on the location of "ocean-island" type sources places a new and significant constraint on compositional layering in the upper mantle, with attendant consequences for the evolution of the upper mantle.

Acknowledgements. We would like to thank the captain and crew of the R/V *Thomas Washington* for their assistance, and in particular, for allowing us to dredge over an active volcano. Thanks also for constructive criticisms from Rick Carlson (DTM), Don DePaolo, and Bob Kay. Marine studies and sampling were supported by NSF grant no. OCE 79-16758 under IDOE.

References

Anderson AT (1982) Parental basalts in subduction zones: Implications for continental evolution. J Geophys Res 87:7047–7060

Arth JG (1976) Behavior of trace elements during magmatic processes: A summary of theoretical models and their application. J Res US Geol Surv 4:41–47

Batiza R (1977) Oceanic crustal evolution: evidence from the petrology and geochemistry of isolated oceanic central volcanoes. PhD thesis, UC San Diego, p 295

Brothers RN (1967) Andesite from Rumble III Volcano, Kermadec Ridge, Southwest Pacific. Bull Volc 31:17–19

Brothers RN, Heming RF, Hawke MM, Davey FJ (1980) Tholeiitic basalt from the Manowai seamount, Tonga-Kermadec ridge. New Zealand J Geol Geophys 23:537–539

Chow TJ, Stern RJ, Dixon TH (1980) Relative and absolute concentrations of K, Rb, Sr and Ba in recent lavas from the Northern Mariana Island Arc. Chem Geol 28:111–121

Cohen RS, Evensen NM, Hamilton PJ, O'Nions RK (1980) U – Pb, Sm – Nd, and Rb – Sr systematics of mid-ocean ridge basalt glasses. Nature 283:149–153

Corwin G, Tracey JI (1965) Marine geologic investigations near the Palau Islands and Guam, Mariana Islands. Int'l Indian Ocean Expedition, USC & GS ship *Pioneer* – 1964, 1:81–90

Danckwerth PA, Newton RC (1978) Experimental determination of the spinel peridotite ot garnet peridotite reaction in the system $MgO-Al_2O_3-SiO_2$ in the range 900–1,100° C and Al_2O_3 isopleths of enstatite in the spinel field. Contrib Mineral Petrol 66:189–201

Delaney JJ, Smith JV, Nixon PH (1979) Model for upper mantle below Malaita, Solomon Islands, deduced from chemistry of lherzolite and megacryst minerals. Contrib Mineral Petrol 70:209–218

DePaolo DJ, Johnson RW (1979) Magma genesis in the New Britain island-arc: Constraints from Nd and Sr isotopes and trace-element patterns. Contrib Mineral Petrol 70:367–379

DePaolo DJ, Wasserburg GJ (1976) Inferences about magma sources and mantle structure from variations of $^{143}Nd/^{143}Nd$. Geophys Res Lett 3:743–746

DePaolo DJ, Wasserburg GJ (1977) The sources of island arcs as indicated by Nd and Sr isotopic studies. Geophys Res Lett 4:465–468

Dixon TH, Batiza R (1979) Petrology and chemistry of recent lavas in the Northern Marianas: Implications for the origin of island arc basalts. Contrib Mineral Petrol 70:167–181

Dixon TH, Stern RJ (1983) Petrology, chemistry, and isotopic composition of submarine volcanoes in the southern Mariana Arc. Geol Soc Am Bull 94:1159–1172

Duncan RA, Compston W (1976) Sr-isotopic evidence for an old mantle source region for French Polynesian volcanism. Geology 4:728–732

Faure G, Assereto R, Tremba EL (1978) Strontium isotopic composition of marine carbonates of Middle Triassic to Early Jurassic age, Lombardic Alps, Italy. Sedimentology 25:523–543

Flanagan EJ (1973) 1972 values for international geochemical reference standards. Geochim Cosmochim Acta 37:1189–1200

Frey FA (1980) The origin of pyroxenites and garnet pyroxenites from Salt Lake Crater, Oahu, Hawaii: Trace element evidence. Am J Sci 280A:427–449

Garcia MO, Liu NWK, Muenow DW (1979) Volatiles in submarine volcanic rocks from the Mariana Island Arc and Through. Geochim Cosmochim Acta 43:305–312

Green DH, Ringwood AE (1967) The genesis of basaltic magmas. Contr Mineral Petrol 15:103–190

Gunn GM (1965) K/Rb and K/Ba ratios in Antarctic and New Zealand tholeiites and alkali basalts. J Geophys Res 70:6241–6247

Hart SR (1971) K, Rb, Cs, Sr and Ba contents and Sr isotope ratios of ocean floor basalts. Phil Trans Roy Soc Long A 268:573–587

Hart SR, Brooks C, Krough TE, Davis GL, Nava D (1970) Ancient and modern volcanic rocks: A trace element model. Earth Planet Sci Lett 10:17–28

Hart SR, Erlank AJ, Kable EJD (1974) Sea floor basalt alteration: Some chemical and Sr isotopic effects. Contrib Mineral Petrol 44:219–230

Hedge CE (1971) Nickel in high-alumina basalts. Geochim Cosmochim Acta 35:522–524

Hedge CE, Peterman ZE, Dickinson WR (1972) Petrogenesis of lavas from Western Samoa. Geol Soc Am Bull 83:2709–2714

Hess HH (1948) Major structural features of the Western North Pacific, An interpretation of H.O. 5485, Bathymetric chart, Korea to New Guinea. Geol Soc Am Bull 59:417–446

Hickey RL, Frey FA (1982) Geochemical characteristics of boninite series volcanics: implications for their source. Geochim Cosmochim Acta 46:2099–2115

Hofmann AW, Wright TL, Feigenson M (1978) Trace elements and Sr isotopes abundances in recent lavas from Kilauea, Hawaii. Carnegie Inst Wash Ybk 77:590–596

Ishizaka K, Carlson RW (1983) Nd–Sr systematics of the Setouchi volcanic rocks, southwest Japan: A clue to the origin of orogenic andesite. Earth Planet Sci Lett 64:327–340

Isshiki N (1958) Petrology of plutonic cognate ejecta from Nishiyama volcano, Hachijo-jima, the Seven Izu Islands, Japan. Jap J Geol and Geogr:55–74

Ito E, Stern RJ (1981) Oxygen- and strontium-isotopic investigations on the origin of volcanism in the Izu-Volcano-Mariana Island Arc. Carnegie Inst Wash Ybk 80:455–461

Ito I, Kennedy GC (1967) Melting and phase relations in a natural peridotite to 40 kilobars. Am J Sci 265:519–528

Jackson ED, Wright TL (1970) Xenoliths in the Honolulu Volcanic Series, Hawaii. J Petrol 11:405–430

Jahn B-M, Bernard-Griffiths I, Charlot R, Cornichet J, Vidal F (1980) Nd and Sr isotopic composition and REE abundances of Cretaceous MORB (Holes 417D and 418A, Legs 51, 52 and 53) Earth Planet Sci Lett 48:171–184

Jakes P, Gill J (1970) Rare earth elements and the island arc tholeiitic series. Earth Planet Sci Lett 9:17–28

Jakes P, White AJR (1972) Major and trace element abundances in volcanic rocks of orogenic areas. Geol Soc Am Bull 83:29–40

Jacques AL, Green DH (1980) Anhydrous melting of peridotite at 0–15 Kb pressure and the genesis of tholeiitic basalts. Contrib Mineral Petrol 73:287–310

Kay RW, Gast PW (1973) The rare earth content and origin of alkali-rich basalts. J Geol 81:653–682

Kushiro I, Shimizu N, Kakamura Y, Akimoto S (1972) Compositions of coexisting liquid and solid phases formed upon melting of natural garnet and spinel lherzolites at high pressures: A preliminary report. Earth Planet Sci Lett 14:19–25

Kushiro I, Syono Y, Akimoto S-I (1968) Melting of a peridotite nodule at high pressures and high water pressures. J Geophys Res 73:6023–6029

Larson EE, Reynolds RL, Merrill R, Levi S, Ozima M, Aoki Y, Kinoshita H, Zasshu S, Kawai N, Nakajima T, Hirooka K (1974) Major-element petrochemistry of some extrusive rocks from the volcanically active Mariana Islands. Bull Volc 38:361–377

MacGregor ID (1964) The reaction 4 enstatite + spinel $\rightleftharpoons$ forsterite + pyrope. Carnegie Inst Wash Ybk 63:156–157

MacGregor ID (1970) The effect of CaO, Cr_2O_3, Fe_2O_3, and Al_2O_3 on the stability of spinel and garnet peridotites. Phys Earth Planet Interiors 3:372–377

MacGregor ID (1974) The system $MgO-Al_2O_3-SiO_2$: Solubility of Al_2O in enstatite for spinel and garnet peridotite compositions. Am Mineral 59:110–119

McCulloch MT, Gregory RT, Wasserburg GJ, Taylor HP (1980) A neodymium, strontium, and oxygen isotopic study of the Cretaceous Samail Ophiolite and implications for the petrogenesis and seawater-hydrothermal alteration of oceanic crust. Earth Planet Sci Lett 46:201–211

McCulloch MT, Wasserburg GJ (1978) Sm–Nd and Rb–Sr chronology of continental crust formation. Science 200:1003–1011

Matsuhisa Y (1979) Oxygen isotopic compositions of volcanic rocks from the East Japan island arc and their bearing on petrogenesis. J Volcanol Geotherm Res 5:271–296

Meijer A (1974) A study of the geochemistry of the Mariana island arc system and its bearing on the genesis and evolution of volcanic arc magmas. PhD thesis, UC Santa Barbara, p 214

Meijer A (1976) Pb and Sr isotopic data bearing on the origin of volcanic rocks from the Mariana island-arc system. Geol Soc Am Bull 87:1358–1369

Meijer A, Reagan M (1981) Petrology and geochemistry of the island of Sarigan in the Mariana Arc; calc-alkaline volcanism in an oceanic setting. Contrib Mineral Petrol 77:337–354

Mysen BO (1974) Phase relations of garnet websterite + H_2O to 30 kbar pressure. Carnegie Inst Wash Ybk 73:240–244

Mysen BO (1978) Experimental determination of rare earth element partitioning between hydrous silicate melt, amphibole, and garnet peridotite minerals at upper mantle pressures and temperatures. Geochim Cosmochim Acta 42:1253–1263

Mysen BO, Boettcher AL (1975a) Melting of a hydrous mantle: I. Phase relations of a natural peridotite at high pressures and temperatures with controlled activities of water, carbon dioxide, and hydrogen. J Petrol 16:520–54

Mysen BO, Boettcher AL (1975b) Melting of a hydrous mantle: II. Geochemistry of crystals and liquids formed by anatexis of mantle peridotite at high pressures and high temperatures as a function of controlled activities of water, hydrogen, and carbon dioxide. J Petrol 16:549–593

Mysen BO, Kushiro I, Nicholls IA, Ringwood AE (1974) A possible mantle origin for andesitic magmas: Discussion of a paper by Nicholls and Ringwood. Earth Planet Sci Lett 21:221–229

Nicholls IA (1974) Liquids in equilibrium with peridotitic mineral assemblages at high water pressures. Contrib Mineral Petrol 45:289–316

Nicholls IA, Harris KL (1980) Experimental rare earth element partition coefficients for garnet, clinopyroxene and amphibole coexisting with andesitic and basaltic liquids. Geochim Cosmochim Acta 44:287–308

Nixon PH, Boyd FR (1979) Garnet bearing lherzolites and discrete nodule suites from the Malaita Alnoite, Solomon Island, S.W. Pacific, and their bearing on oceanic mantle composition and geotherm. In: Boyd FR, Meyer HOA (eds) The Mantle Sample: Inclusions in kimberlites and other volcanics. Proc 2nd Int Kimberlite Conf, Am Geophys Union 2:400–423

Obata M (1976) The solubility of Al_2O_3 in orthopyroxenes in spinel

and plagioclase peridotites and spinel pyroxenite. Am Mineral 61:804–816
O'Neil JR, Hedge CE, Jackson ED (1970) Isotopic investigations of xenoliths and host basalts from the Honolulu Volcanic Series. Earth Planet Sci Lett 8:253–257
O'Nions RK, Carter SR, Cohen RS, Evensen NM, Hamilton PJ (1978) Pb, Nd, and Sr isotopes in oceanic ferromanganese deposits and ocean floor basalts. Nature 273:435–438
O'Nions RK, Hamilton PJ, Evenson NM (1977) Variations in $^{143}Nd/^{144}Nd$ and $^{87}Sr/^{86}Sr$ in oceanic basalts. Earth Planet Sci Lett 34:13–22
Pearce JA, Cann JR (1973) Tectonic settings of basic volcanic rocks determined using trace element analyses. Earth Planet Sci Lett 19:290–300
Peipgras DJ, Wasserburg GJ, Dasch EJ (1980) The isotopic composition of Nd in different ocean masses. Earth Planet Sci Lett 45:233–236
Philpotts JA, Schnetzler CC (1970) Phenocryst-matrix partition coefficients for K, Rb, Sr and Ba, with applications to anorthosite and basalt genesis. Geochim Cosmochim Acta 34:307–322
Richard P, Shimizu N, Allegre CJ (1976) $^{143}Nd/^{144}Nd$, a natural tracer: An application to oceanic basalts. Earth Planet Sci Lett 31:269–278
Ringwood AE (1966) The chemical composition and origin of the earth. In: PM Hurley (ed) Advances in Earth Science, pp 287–356
Ronck R (1975) Volcano erupting near Tinian. Pacific Daily News, April 30, 1975:3
Shaw DM (168) A review of K – Rb fractionation trends by covariance analysis. Geochim Cosmochim Acta 32:573–601
Shimamura H, Asada T (1976) Apparent velocity measurements on an oceanic lithosphere. Physics Earth Planet Interiors 13:15–22
Shimamura H, Asada T, Kimazawa M (1977) High shear velocity layer in the upper mantle of the Western Pacific. Nature 269:680–682
Shimizu N (1974a) An isotopic dilution technique for analysis of the rare earth elements. Carnegie Inst Wash Ybk 73:941–943
Shimizu N (1974b) An experimental study of the partitioning of K, Rb, Cs, Sr, and Ba between clinopyroxene and liquid at high pressures. Geochim Cosmochim Acta 38:1789–1798
Stern RJ (1979) On the origin of andesite in the Northern Mariana island arc: Implications from Agrigan. Contrib Mineral Petrol 68:207–219
Stern RJ (1981) A common mantle source for western Pacific island arc and "hot spot" magmas – implications for layering in the upper mantle. Carnegie Inst Wash Ybk 80:455–461
Stern RJ (1982) Strontium isotopes from circum-Pacific intra-oceanic island arcs and marginal basins: Regional variations and implications for magmagenesis. Geol Soc Am Bull 93:477–486
Stern RJ, Bibee LD (1980) Esmeralda Bank: Geochemistry of an active submarine volcano in the Mariana Island Arc and its implications for magmagenesis in island arcs. Carnegie Inst Wash Ybk 79:465–472
Takahahsi E (1978) Petrologic model of the crust and upper mantle of the Japanese Island Arcs. Bull Volc 41:529–547
Taylor SR, Kaye M, White ARJ, Duncan AR, Ewart A (1969) Genetic significance of Co, Cr, Ni, Sc, and V content of andesites. Geochim Cosmochim Acta 33:275–286
Tracy RJ (1980) Petrology and genetic significance of an ultramafic xenolith suite from Tahiti. Earth Planet Sci 48:80–96
White WH, Hofmann AW (1982) Sr and Nd isotope geochemistry of oceanic basalts and mantle evolution. Nature 296:821–825
Wood DA, Marsh NG, Tarney J, Joron J-L, Fryer P, Treuil M (1981) Geochemistry of igneous rocks recovered from a transect across the Mariana Trough, arc, fore-arc, and trench, sites 453 through 461, Deep Sea Drilling Project Leg 60. In: Hussong DM (ed) Init Repts DSDP 60:611–633
Zindler A, Hart SR, Frey FA, Jakobsson SP (1979) Nd and Sr isotope ratios and rare earth element abundances in Reykjanes Peninsula basalts: Evidence for mantle heterogeneity beneath Iceland. Earth Planet Sci Lett 45:249–262

Received April 6, 1981; Accepted December 19, 1983